Meccanica (2015) 50:2077–2091
DOI 10.1007/s11012-015-0136-x

Deformation of a rotating two-temperature generalized-magneto thermoelastic medium with internal heat source due to hydrostatic initial stress

Samia M. Said

Received: 22 October 2014 / Accepted: 19 February 2015 / Published online: 27 February 2015

Abstract The three-phase-lag model and Green–Naghdi theory without energy dissipation are employed to study the deformation of a two-temperature generalized-magneto thermoelastic medium with an internal heat source that is moving with a constant speed under the hydrostatic initial stress and the rotation. Normal mode analysis is used to obtain the analytical expressions of the displacement components, force stress, thermal temperature and conductive temperature. The numerical results are given and presented graphically when mechanical force is applied. Comparisons are made with the results of the two models for two different values of the hydrostatic initial stress. Also, comparisons are made with results of the two models with and without the rotation as well as the two-temperature.

Keywords Conductive temperature · Green–Naghdi theory · Hydrostatic initial stress · Rotation · Thermal temperature · Three-phase-lag mode

S. M. Said
Department of Mathematics, Faculty of Science, Zagazig University, P.O. Box 44519, Zagazig, Egypt

S. M. Said (✉)
Department of Mathematics, Faculty of Science and Arts, Qassim University, P.O. Box 6666, Buraidah 51452, Al-mithnab, Kingdom of Saudi Arabia
e-mail: samia_said59@yahoo.com

1 Introduction

Biot [1] formulated the coupled thermoelasticity theory to eliminate the paradox inherent in the classical uncoupled theory that the elastic deformation has no effect on the temperature. The field equations for the both theories are of a mixed parabolic-hyperbolic type, which predict infinite speeds for thermoelastic singals, contrary to physical observations. During the last three decades, generalized theories involving a finite speed of heat transportation (hyperbolic heat transport equation) in elastic solids have been developed to remove this paradox. The first generalization is proposed by Lord and Shulman [2] and is known as the extended thermoelasticity theory which involves one thermal relaxation time parameter (single-phase-lag model). The second generalization of the coupled thermoelasticity theory is developed by Green and Lindsay [3], which involving two relaxation times is known as temperature rate dependent thermoelasticity. The third generalization is known as low-temperature thermoelasticity introduced by Hetnarski and Ignaczak [4] called H–I theory. The fourth generalization is concerned with the thermoelasticity without energy dissipation and thermoelasticity with energy dissipation introduced by Green and Naghdi [5–7] and provide sufficient basic modifications in the constitutive equations that permit treatment of a much wider class of heat flow problems, labeled as types I, II, III. The nature of these three types of constitutive equations is such that when the respective theories are

linearized, type-I is the same as the classical heat equation, whereas the linearized versions of type-II and type-III theories permit the propagation of thermal waves at finite speed. The fifth generalization of the thermoelasticity theory is known as the dual-phase-lag thermoelasticity developed by Tzou [8] and Chandrasekhariah [9]. Tzou considered micro-structural effects in the delayed response in time in the macroscopic formulation by taking into account that increase of the lattice temperature is delayed due to photon-electron interactions on the macroscopic level. Tzou [8] introduced two-phase-lag to both the heat flux vector and the temperature gradient. According to this model, classical Fourier's law $\boldsymbol{q} = -K\nabla \mathrm{T}$ has been replaced by $\boldsymbol{q}(\mathrm{P}, \mathrm{t} + \tau_{\mathrm{q}}) = -K\nabla \mathrm{T}(\mathrm{P}, \mathrm{t} + \tau_{\mathrm{T}})$, where the temperature gradient $\nabla \mathrm{T}$ at a point P of the material at time $\mathrm{t} + \tau_{\mathrm{T}}$ corresponds to the heat flux vector $\boldsymbol{q}$ at the same point at time $\mathrm{t} + \tau_{\mathrm{q}}$. Here K is the thermal conductivity of the material. The delay time τ_{T} is interpreted as that caused by the micro-structural interactions and is called the phase-lag of the temperature gradient. The other delay time τ_{q} is interpreted as the relaxation time due to the fast transient effects of thermal inertia and is called the phase-lag of the heat flux. Recently Choudhuri [10] has proposed a theory with three-phase lag (**3PHL**) which is able to contain all the previous theories at the same time. In this case Fourier's law $\boldsymbol{q} = -K\nabla \mathrm{T}$ has been replaced by $\boldsymbol{q}(\mathrm{P}, \mathrm{t} + \tau_{\mathrm{q}}) = -[K\nabla \mathrm{T}(\mathrm{P}, \mathrm{t} + \tau_{\mathrm{T}}) + K^{*}\nabla v(\mathrm{P}, \mathrm{t} + \tau_{v})]$, where ∇v $(\dot{v} = T)$ is the thermal displacement gradient and K^{*} is the additional material constant and τ_{v} is the phase-lag for the thermal displacement gradient. The purpose of the work of Choudhuri [10] was to establish a mathematical model that includes (**3PHL**) in the heat flux vector, the temperature gradient and in the thermal displacement gradient. For this model, we can consider several kinds of Taylor approximations to recover the previously cited theories. In particular the models of Green and Naghdi are recovered. Quintanilla and Racke [11] are introduced a note on the stability in three-phase-lag heat conduction. Kar and Kanoria [12] studied a thermo-visco-elastic problem of a spherical shell in the context of **3PHL** model. Quintanilla [13] discussed the spatial behavior of solutions of **3PHL** heat equations. Kanoria and Mallik [14] studied a generalized thermo—visco-elastic interaction due to a periodically varying heat source with **3PHL** effect. Abbas [15] discussed the **3PHL** model on a thermoelastic interaction in an unbounded fiber-reinforced anisotropic medium with a cylindrical cavity. The two dimensional problem of a magneto-thermoelasticity fiber-reinforced medium under temperature dependent properties with the **3PHL** model was presented by Othman and Said [16].

A theory of the heat conduction in deformable bodies which depends upon two distinct temperatures, the conductive temperature and the thermodynamic temperature, has been established by Chen and Gurtin [17] and Chen et al. [18, 19]. To time-independent problems, the difference between these two distinct temperatures is proportional to the heat supply and in the absence of any heat supply, these two-temperature are identical as Chen et al. [18]. For time-dependent situations and for wave propagation problems, in particular, the two-temperature are in general different, regardless of the presence of a heat supply. Warren and Chen [20] investigated the wave propagation in the two-temperature theory of thermoelasticity. Youssef [21] has proposed a theory in the context of the generalized theory of thermoelasticity with two-temperature. The propagation of harmonic plane waves in the media described by the two-temperature theory of thermoelasticity is investigated by Puri and Jordan [22]. Several problems with the two-temperature theory of thermoelasticity have been solved by Abbas and Youssef [23], Kumar and Mukhopadhyay [24], Das and Kanoria [25], Abbas and Zenkour [26] and Othman et al. [27] etc.

The investigation of the interaction between the magnetic field, stress, and strain in a thermoelastic solid is very important due to its many applications in the field of geophysics, plasma physics and related topics, especially in the nuclear field, where the extremely high temperature and temperature gradients, as well as the magnetic fields originating inside nuclear reactors, influence their design and operations. The theory of magneto-thermoelasticity is concerned with the influence of a magnetic field on the elastic and thermoelastic deformations of solid bodies. This theory has aroused much interest in recent years, because of its applications in various branches of science and technology. The development of the interaction of an electromagnetic field, thermal field, and elastic field is available in many studies [28–32]. Biot [1] showed the acoustic propagation under initial

stress, which is fundamentally different from that under a stress-free state. Montanaro [33] investigated the isotropic linear thermoelasticity with a hydrostatic initial stress. Ahmed [34] studied the effect of an initial stress on the propagation of Rayleigh waves in a granular medium under incremental thermal stresses. Othman and Said [35] discussed the effect of a mechanical force on the generalized thermoelasticity in a fiber-reinforced under three theories.

The present paper is concerned with the investigations related to the effect of a hydrostatic initial stress and a rotation with the **3PHL** and thermoelasticity without energy dissipation (**G-N II**) models on a two-temperature magneto-thermoelastic medium with an internal heat source that is moving with a constant speed by applying normal mode analysis. The variations of the considered variables with the horizontal distance are illustrated graphically. Comparisons are made between the results of the two models for two different values of a hydrostatic initial stress. Also, comparisons are made with results of the two models with and without the rotation as well as the two-temperature.

2 Formulation of the problem and basic equations

We consider the problem of a rotating thermoelastic half-space with an internal heat source that is moving with a constant speed ($x \geq 0$). The generalized thermoelastic medium is permeated into a uniform magnetic field with constant intensity $H = (0, H_0, 0)$ which is acting parallel to the y-axis and under the effect of a hydrostatic initial stress. We are interested in a plane strain in the xz-plane [displacement components $u = (u, 0, v)$], $\frac{\partial}{\partial y} = 0$. When all body forces are neglected the governing equations are

1. The constitutive equations of the theory of generalized thermoelasticity are given as in [33]

$$\sigma_{ij} = \lambda\, e_{kk}\delta_{ij} + 2\mu\, e_{ij} - \gamma\, \hat{T}\, \delta_{ij} - P\,(\,\omega_{ij} + \delta_{ij}\,), \tag{2.1}$$

$$\omega_{ij} = \frac{1}{2}(u_{j,i} - u_{i,j}). \tag{2.2}$$

where σ_{ij} are the components of stress, e_{ij} are the components of strain, e_{kk} is the dilatation, λ, μ are elastic constants, $\gamma = (\,3\lambda + 2\mu\,)\alpha_t$, α_t is the thermal expansion coefficient, $\hat{T} = T - T_0$, where T is the temperature above the reference temperature T_0, δ_{ij} is the Kronecker's delta and P is the initial pressure. The strains can be expressed in terms of the displacement u_i as

$$e_{ij} = \frac{1}{2}(u_{i,j} + u_{j,i}), \qquad e_{kk} = u_{k,k} \quad i.j,\, k = x,\, z \tag{2.3}$$

Equation (2.1), then yields

$$\sigma_{xx} = A\frac{\partial u}{\partial x} + \lambda\, \frac{\partial v}{\partial z} - \gamma\hat{T} - P, \tag{2.4}$$

$$\sigma_{zz} = \lambda\, \frac{\partial u}{\partial x} + A\, \frac{\partial v}{\partial z} - \gamma\hat{T} - P, \tag{2.5}$$

$$\sigma_{xz} = S_1\frac{\partial u}{\partial z} + S_2\frac{\partial v}{\partial x}, \qquad \sigma_{zx} = S_2\frac{\partial u}{\partial z} + S_1\frac{\partial v}{\partial x}, \tag{2.6}$$

where $A = \lambda + 2\mu,\ S_1 = \mu + \frac{P}{2},\ S_2 = \mu - \frac{P}{2}$.

2. The dynamical equations of a rotating magneto-thermoelastic medium are given by Schoenberg and Censor [36]

$$\rho\,[\ddot{u}_i + \{\underline{\Omega} \wedge (\underline{\Omega} \wedge \underline{u})\}_i + 2(\underline{\Omega} \wedge \dot{\underline{u}})_i] = \sigma_{ij,j} + F_i, \quad i, j = 1, 2, 3. \tag{2.7}$$

where $\underline{\Omega} = \Omega\,\underline{\hat{n}}$ is an angular velocity of the rotating medium, $\underline{\hat{n}}$ is a unit vector representing the direction of the axis of rotation and F_i is the Lorentz force and is given in the form $F_i = \mu_0\,(\underline{J} \wedge \underline{H})_i$. The variations of the magnetic and electric fields are perfectly conducting slowly moving medium and are given by Maxwell's equation in [30]

$$\underline{J} = curl\,\underline{h} - \varepsilon_0\,\dot{\underline{E}}, \quad curl\,\underline{E} = -\mu_0\dot{\underline{h}}, \quad \underline{E} = -\mu_0\,(\dot{\underline{u}} \wedge \underline{H}), \quad \underline{\nabla} \cdot \underline{h} = 0, \tag{2.8}$$

where μ_0 is the magnetic permeability, ε_0 is the electric permeability, $\underline{J}$ is the current density vector, $\dot{\underline{u}}$ is the particle velocity of the medium, and the small effect of the temperature gradient on $\underline{J}$ is also ignored. The dynamic displacement vector is actually measured from a steady-state deformed position and the deformation is assumed to be small. Due to the

application of the initial magnetic field $\underline{H}$, there are an induced magnetic field $\underline{h} = (0, h, 0)$ and an induced electric field $\underline{E}$, as well as the simplified equations of electrodynamics of a slowly moving medium for a homogeneous, thermal and electrically conducting, elastic solid. Expressing the components of the vector $\underline{J} = (J_1, J_2, J_3)$ in terms of displacement by eliminating the quantities $\underline{h}$ and $\underline{E}$ from Eqs. (2.8), we get $J_1 = -\frac{\partial h}{\partial z} - \mu_0 \varepsilon_0 H_0 \ddot{v}$, $J_2 = 0$, $J_3 = \frac{\partial h}{\partial x} + \mu_0 \varepsilon_0 H_0 \ddot{u}$, thus yields

$$F_1 = -\mu_0 H_0 \frac{\partial h}{\partial x} - \varepsilon_0 \mu_0^2 H_0^2 \frac{\partial^2 u}{\partial t^2}, \quad F_2 = 0, \\ F_3 = -\mu_0 H_0 \frac{\partial h}{\partial z} - \varepsilon_0 \mu_0^2 H_0^2 \frac{\partial^2 v}{\partial t^2}. \tag{2.9}$$

From Eqs. (2.4)–(2.6) and (2.9) into Eq. (2.7) and using the summation convection, we note that the third equation of motion in Eq. (2.7) is identically satisfied and the first two equations become

$$\rho \left(\frac{\partial^2 u}{\partial t^2} - \Omega^2 u + 2\Omega \dot{v} \right) = A \frac{\partial^2 u}{\partial x^2} + B \frac{\partial^2 v}{\partial x \partial z} + S_1 \frac{\partial^2 u}{\partial z^2} - \gamma \frac{\partial \hat{T}}{\partial x} - \mu_0 H_0 \frac{\partial h}{\partial x} - \varepsilon_0 \mu_0^2 H_0^2 \frac{\partial^2 u}{\partial t^2}, \tag{2.10}$$

$$\rho \left(\frac{\partial^2 v}{\partial t^2} - \Omega^2 v - 2\Omega \dot{u} \right) = S_1 \frac{\partial^2 v}{\partial x^2} + B \frac{\partial^2 u}{\partial x \partial z} + A \frac{\partial^2 v}{\partial z^2} - \gamma \frac{\partial \hat{T}}{\partial z} - \mu_0 H_0 \frac{\partial h}{\partial z} - \varepsilon_0 \mu_0^2 H_0^2 \frac{\partial^2 v}{\partial t^2}, \tag{2.11}$$

where $B = \lambda + S_2$.

3. The generalized heat conduction equation in the **3PHL** model with two-temperature is given by [10, 21]

$$K^* \nabla^2 \Phi + \tau_v^* \nabla^2 \dot{\Phi} + K \tau_T \nabla^2 \ddot{\Phi} = \left(1 + \tau_q \frac{\partial}{\partial t} + \frac{1}{2} \tau_q^2 \frac{\partial^2}{\partial t^2} \right) (\rho C_E \ddot{T} + \gamma T_0 \ddot{e} - Q). \tag{2.12}$$

The relation between the conductive temperature and the thermodynamics temperature is

$$\Phi - T = \delta \Phi_{,ii}, \tag{2.13}$$

where K^* is the coefficient of thermal conductivity, K is the additional material constant, ρ is the mass density, C_E is the specific heat at constant strain, Q is a moving internal heat source, Φ is the conductive temperature, $\delta > 0$ a constant called two-temperature parameter, τ_T and τ_q are the phase-lag of temperature gradient and the phase-lag of heat flux respectively. Also $\tau_v^* = K + \tau_v K^*$, where τ_v is the phase-lag of thermal displacement gradient. Equations (2.10)–(2.12), when $K = \tau_T = \tau_q = \tau_v = 0$, reduce to the equations of thermoelasticity without energy dissipation (**GN-II**) theory. In the above equations a dot denotes differentiation with respect to time, and a comma followed by a suffix denotes partial derivative with respect to the corresponding coordinates.

Introducing the following non-dimension quantities:

$$(x', z', u', v') = c_1 \eta (x, z, u, v), \quad (t', \tau_q', \tau_v', \tau_T') = c_1^2 \eta (t, \tau_q, \tau_v, \tau_T), \quad \Omega' = \frac{\Omega}{c_1^2 \eta}, \\ \theta = \frac{\gamma \hat{T}}{(\lambda + 2\mu)}, \quad \Phi' = \frac{\gamma (\Phi - T_0)}{(\lambda + 2\mu)}, \quad \sigma_{ij}' = \frac{\sigma_{ij}}{\mu}, \\ Q' = \frac{\gamma Q}{\rho C_E c_1^4 \eta^2 (\lambda + 2\mu)}, \\ h' = \frac{h}{H_0}, \quad i, j = 1, 2. \tag{2.14}$$

where $\eta = \frac{\rho C_E}{K^*}$, $c_1^2 = \frac{(\lambda + 2\mu)}{\rho}$.

Using the above non-dimension variables, then employing $h = -H_0 e$, Eqs. (2.10)–(2.13) take the following form (dropping the primes for convenience)

$$\alpha \frac{\partial^2 u}{\partial t^2} - \Omega^2 u + 2\Omega \dot{v} = A_{11} \frac{\partial^2 u}{\partial x^2} + B_{11} \frac{\partial^2 v}{\partial x \partial z} + S_{11} \frac{\partial^2 u}{\partial z^2} - \frac{\partial \theta}{\partial x}, \tag{2.15}$$

$$\alpha \frac{\partial^2 v}{\partial t^2} - \Omega^2 v - 2\Omega \dot{u} = S_{11} \frac{\partial^2 v}{\partial x^2} + B_{11} \frac{\partial^2 u}{\partial x \partial z} + A_{11} \frac{\partial^2 v}{\partial z^2} - \frac{\partial \theta}{\partial z}, \tag{2.16}$$

$$C_K\Phi_{,ii} + C_v\dot{\Phi}_{,ii} + C_T\ddot{\Phi}_{,ii} = \left(1 + \tau_q\frac{\partial}{\partial t} + \frac{1}{2}\tau_q^2\frac{\partial^2}{\partial t^2}\right)(\ddot{\theta} + \varepsilon\ddot{e} - Q), \tag{2.17}$$

$$\Phi - \theta = \beta_0\Phi_{,ii}, \tag{2.18}$$

where, $A_{11} = A_1 + h_0H_0$, $B_{11} = B_1 + h_0H_0$, $(A_1, B_1, S_{1_1}, h_0) = \frac{(A,B,S_1,\mu_0H_0^2)}{\rho c_1^2}$, $C_K = \frac{K^*}{\rho C_E c_1^2}$, $C_v = \frac{\eta K}{\rho C_E} + C_K\tau_v$, $C_T = \frac{\eta K\tau_T}{\rho C_E}$, $\varepsilon = \frac{\gamma^2 T_0}{\rho C_E(\lambda+2\mu)}$, $\alpha = 1 + \frac{\varepsilon_0\mu_0^2H_0^2}{\rho}$, $\beta_0 = \delta c_1^2\eta^2$.

3 Normal mode analysis

The solution of the considered physical variable can be decomposed in terms of normal modes as the following form:

$$[u, v, \theta, \Phi, \sigma_{ij}](x, z, t) = [u^*, v^*, \theta^*, \Phi^*, \sigma_{ij}^*](x)\exp(\omega t + ibz),$$

$$Q = Q^*\exp(\omega t + ibz), \quad Q^* = Q_0v_0, \tag{3.1}$$

where ω is a complex constant, $i = \sqrt{-1}$, b is the wave number in the z-direction, v_0 is the velocity of a moving internal heat source and Q_0 is the magnitude of an internal heat source. $u^*(x), v^*(x), \theta^*(x), \Phi^*(x)$, and $\sigma_{ij}^*(x)$ are the amplitudes of the field quantities.

Substituting from Eqs. (3.1) in Eqs. (2.15)–(2.18), we get

$$[A_{11}\mathrm{D}^2 - N_1]u^* + [ibB_{11}\mathrm{D} - 2\Omega\omega]\,v^* = \mathrm{D}\theta^*, \tag{3.2}$$

$$[ibB_{11}\mathrm{D} + 2\Omega\omega]\,u^* + [S_{11}\mathrm{D}^2 - N_2]v^* = ib\theta^*, \tag{3.3}$$

$$\varepsilon N_3\mathrm{D}u^* + i\varepsilon bN_3v^* + N_3\theta^* = [N_4\mathrm{D}^2 - N_5]\Phi^* + N_0Q_0v_0, \tag{3.4}$$

$$\theta^* = (1 + \beta_0b^2 - \beta_0\mathrm{D}^2)\Phi^*, \tag{3.5}$$

where

$$N_1 = S_{11}b^2 + \alpha\omega^2 - \Omega^2,$$

$$N_2 = A_{11}b^2 + \alpha\omega^2 - \Omega^2,$$

$$N_3 = \omega^2\left(1 + \tau_q\omega + \frac{1}{2}\tau_q^2\omega^2\right),$$

$$N_4 = C_K + C_v\omega + C_T\omega^2,$$

$$N_5 = N_4b^2.$$

Introducing Eq. (3.5) in Eqs. (3.2)–(3.4), we get

$$[A_{11}\mathrm{D}^2 - N_1]\,u^* + [ibB_{11}\mathrm{D} - 2\Omega\omega]\,v^* = \mathrm{D}\,(N_8 - \beta_0\mathrm{D}^2)\Phi^*, \tag{3.6}$$

$$[ibB_{11}\mathrm{D} + 2\Omega\omega]\,u^* + [S_{11}\mathrm{D}^2 - N_2]v^* = ib\,(N_8 - \beta_0\mathrm{D}^2)\Phi^*, \tag{3.7}$$

$$\varepsilon N_3\mathrm{D}u^* + i\varepsilon bN_3v^* = [N_6\mathrm{D}^2 - N_7]\Phi^* + N_0Q_0v_0, \tag{3.8}$$

where

$$N_6 = N_4 + N_3\beta_0,$$

$$N_7 = N_5 + N_3N_8,$$

$$N_8 = 1 + \beta_0b^2,$$

$$\mathrm{D} = \frac{\mathrm{d}}{\mathrm{d}x}.$$

Eliminating $v^*(x)$ and $\Phi^*(x)$ between Eqs. (3.6)–(3.8), we obtain the sixth-order ordinary differential equation satisfied with $u^*(x)$,

$$\left[\mathrm{D}^6 - L\mathrm{D}^4 + L_1\mathrm{D}^2 - L_2\right]u^*(x) = -\frac{2ib\Omega\omega N_0N_8Q_0v_0}{L_3}, \tag{3.9}$$

where

$$L = \frac{L_4}{L_3},$$

$$L_1 = \frac{L_5}{L_3},$$

$$L_2 = \frac{L_6}{L_3},$$

$$L_3 = (A_{11}\,N_6 + \varepsilon\,N_3\,\beta_0)\,S_{11},$$

$$L_4 = A_{11}N_2N_6 + A_{11}N_7S_{11} + b^2\varepsilon N_3\beta_0A_{11} + N_1N_6S_{11} - b^2B_{11}^2N_6 - 2b^2\varepsilon N_3\beta_0B_{11} + \varepsilon N_3N_2\beta_0 + \varepsilon N_3N_8S_{11},$$

$$L_5 = A_{11}N_2N_7 + b^2\varepsilon N_3N_8A_{11} - 2b^2\varepsilon N_3N_8B_{11} + N_1N_2N_6 + S_{11}N_1N_7 + b^2\varepsilon N_3N_1\beta_0 + 4\Omega^2\omega^2N_6 - b^2B_{11}^2N_7 + \varepsilon N_3N_2N_8,$$

$$L_6 = N_1N_2N_7 + b^2\varepsilon N_3N_8N_1 + 4\Omega^2\omega^2N_7.$$

In a similar manner, we can show that $v^*(x)$ and $\Phi^*(x)$ satisfy the equations,

$$\left[\mathrm{D}^6 - L\mathrm{D}^4 + L_1\mathrm{D}^2 - L_2\right] v^*(x) = \frac{ibN_0N_1N_8Q_0v_0}{L_3}, \tag{3.10}$$

$$\left[\mathrm{D}^6 - L\mathrm{D}^4 + L_1\mathrm{D}^2 - L_2\right] \Phi^*(x) = -\frac{(4\Omega^2\omega^2 + N_1N_2)\,N_0\,Q_0v_0}{L_3}, \tag{3.11}$$

Equation (3.9) can be factored as

$$\left(\mathrm{D}^2 - k_1^2\right)\left(\mathrm{D}^2 - k_2^2\right)\left(\mathrm{D}^2 - k_3^2\right) u^*(x) = -\frac{2i\,b\Omega\omega N_0N_8Q_0v_0}{L_3}, \tag{3.12}$$

where $k_n^2 (n = 1, 2, 3)$ are the roots of the following characteristic equation:

$$k^6 - Lk^4 + L_1k^2 - L_2 = 0.$$

The solution of Eq. (3.9), which is bounded as $x \to \infty$, is given by

$$u^*(x) = \sum_{n=1}^{3} M_n(b,\omega)\,\exp(-k_nx) + \frac{2ib\,\Omega\omega N_0N_8Q_0v_0}{L_3\,L_2}. \tag{3.13}$$

In a similar manner, we get that

$$v^*(x) = \sum_{n=1}^{3} H_{1n}M_n(b,\omega)\exp(-k_nx) - \frac{ibN_0N_1N_8Q_0v_0}{L_3L_2}, \tag{3.14}$$

$$\Phi^*(x) = \sum_{n=1}^{3} H_{2n}M_n(b,\omega)\,\exp(-k_nx) + \frac{(4\Omega^2\omega^2 + N_1N_2)\,N_0\,Q_0v_0}{L_3\,L_2}. \tag{3.15}$$

where

$$H_{1n} = \frac{ib\left[(A_{11} - B_{11})\,k_n^2 - N_1\right] + 2\Omega\omega k_n}{-S_{11}k_n^3 + (N_2 - b^2B_{11})\,k_n + 2ib\Omega\omega},$$

$$H_{2n} = \frac{A_{11}k_n^2 - N_1 - (\mathrm{i}bB_{11}k_n + 2\Omega\omega)H_{1n}}{-N_8\,k_n + \beta_0\,k_n^3}.$$

Introducing Eq. (3.15) in Eq. (3.5), this yields

$$\theta^*(x) = \sum_{n=1}^{3} H_{3n}M_n(b,\omega)\,\exp(-k_nx) + \frac{(4\Omega^2\omega^2 + N_1N_2)\,N_0\,N_8\,Q_0v_0}{L_3\,L_2} \tag{3.16}$$

where

$$H_{3n} = (N_8 - \beta_0k_n^2)\,H_{2n}.$$

Substituting from Eqs. (2.14) and (3.1) in Eqs. (2.4)–(2.6), we get

$$\mu\sigma_{xx}^* = A\mathrm{D}u^* + ib\lambda v^* - (\lambda + 2\mu)\,\theta^* - P^*, \tag{3.17}$$

$$\mu\sigma_{zz}^* = \lambda\mathrm{D}u^* + ibAv^* - (\lambda + 2\mu)\,\theta^* - P^*, \tag{3.18}$$

$$\mu\sigma_{xz}^* = ibS_1u^* + S_2\mathrm{D}v^*, \quad \mu\sigma_{zx}^* = ibS_2u^* + S_1\mathrm{D}v^*. \tag{3.19}$$

Introducing Eqs. (3.13), (3.14) and (3.16) in Eqs. (3.17)–(3.19), this yields

$$\sigma_{xx}^* = \sum_{n=1}^{3} H_{4n}M_n(b,\omega)\,\exp(-k_nx) + G_1, \tag{3.20}$$

$$\sigma_{zz}^* = \sum_{n=1}^{3} H_{5n}M_n(b,\omega)\,\exp(-k_nx) + G_2, \tag{3.21}$$

$$\sigma_{xz}^{*} = \sum_{n=1}^{3} H_{6n} M_n(b,\omega)\, \exp(-k_n x) - G_3, \tag{3.22}$$

where

$$H_{4n} = \frac{1}{\mu}\left[-Ak_n + ib\lambda H_{1n} - (\lambda + 2\mu) H_{3n}\right],$$

$$H_{5n} = \frac{1}{\mu}\left[ibAH_{1n} - \lambda k_n - (\lambda + 2\mu) H_{3n}\right],$$

$$H_{6n} = \frac{1}{\mu}(ibS_1 - S_2 k_n H_{1n}),$$

$$G_1 = \frac{[b^2\lambda N_1 - (\lambda + 2\mu)(4\Omega^2\omega^2 + N_1 N_2)] N_0 N_8 Q_0 v_0}{\mu L_3 L_2} - \frac{P^*}{\mu},$$

$$G_2 = \frac{[b^2 A N_1 - (\lambda + 2\mu)(4\Omega^2\omega^2 + N_1 N_2)] N_0 N_8 Q_0 v_0}{\mu L_3 L_2} - \frac{P^*}{\mu},$$

$$G_3 = \frac{2b^2\Omega\omega N_0 N_8 S_1 Q_0 v_0}{\mu L_3 L_2}.$$

4 Boundary condition

In this section we determine the parameters $M_n (n = 1, 2, 3)$. In the physical problem, we should suppress the positive exponentials that are unbounded at infinity. The constants M_1, M_2, M_3 have to be chosen such that the boundary conditions on the surface at $x = 0$ take the form

$$\frac{\partial \Phi}{\partial x} = 0, \quad \sigma_{xx} = f(z,t) = -R_P f^* \exp(\omega t + ibz), \quad \sigma_{xz} = 0 \tag{4.1}$$

$f(z, t)$ is arbitrary functions of z, t. f^* is constant and R_P is the magnitude of a hydrostatic initial stress. Using the expressions of the variables considered into the above boundary conditions [Eq. (4.1)], we can obtain the following equations satisfied with the parameters:

$$-\sum_{n=1}^{3} k_n H_{2n} M_n = 0, \quad \sum_{n=1}^{3} H_{4n} M_n = -R_P - G_1, \quad \sum_{n=1}^{3} H_{7n} M_n = G_3. \tag{4.2}$$

Solving the above system of Eqs. (4.2), we obtain a system of three equations. After applying the inverse of matrix method, we have the values of the three constants M_n $(n = 1, 2, 3)$. Hence, we obtain the expressions of displacements, thermal temperature, conductive temperature and the stress components.

$$\begin{pmatrix} M_1 \\ M_2 \\ M_3 \end{pmatrix} = \begin{pmatrix} k_1 H_{21} & k_2 H_{22} & k_3 H_{23} \\ H_{41} & H_{42} & H_{43} \\ H_{71} & H_{72} & H_{73} \end{pmatrix}^{-1} \begin{pmatrix} 0 \\ -R_P - G_1 \\ G_3 \end{pmatrix}$$

5 Numerical calculation and discussion

With a view to illustrating the analytical procedure presented earlier, we now consider a numerical example for which computational results are given, to compare these in the context of the **3PHL** and the thermoelasticity without energy dissipation (**GN-II**) theory, and to study the effect of rotation and a hydrostatic initial stress on the wave propagation in a two-temperature generalized-magneto thermoelastic medium, we now present some numerical results for the physical constants as [16].

$\lambda = 7.76 \times 10^9\,\mathrm{N\,m^{-2}}$, $\mu = 3.86 \times 10^{10}\,\mathrm{N\,m^{-2}}$, $\rho = 8954\,\mathrm{kg\,m^{-3}}$, $C_E = 383.1\,\mathrm{J\,kg^{-1}\,K^{-1}}$,

$\tau_T = 7 \times 10^{-5}\,\mathrm{s}$, $\tau_q = 9 \times 10^{-5}\mathrm{s}$, $\tau_v = 6 \times 10^{-5}\,\mathrm{s}$, $\alpha_t = 3.78 \times 10^{-4}\,\mathrm{K^{-1}}$, $K^* = 386\,\mathrm{w\,m^{-1}\,K^{-1}}$,

$K = 150\,\mathrm{w\,m^{-1}\,K^{-1}}$, $\omega = \omega_0 + i\xi$, $\omega_0 = 0.8$, $\xi = 0.5$, $Q_0 = 3\,\mathrm{K}$, $v_0 = 0.5\,\mathrm{m\,s^{-1}}$,

$H_0 = 100$, $P = 5\,\mathrm{N.\,m^{-2}}$, $b = 0.3$, $\varepsilon_0 = 0.7$, $\mu_0 = 2.5$, $f^* = 1.0$, $R_P = 0.9, 3.5$,

$T_0 = 273\,\mathrm{K}$, $\delta = 3 \times 10^{-15}$, $\Omega = 0, 2.5$.

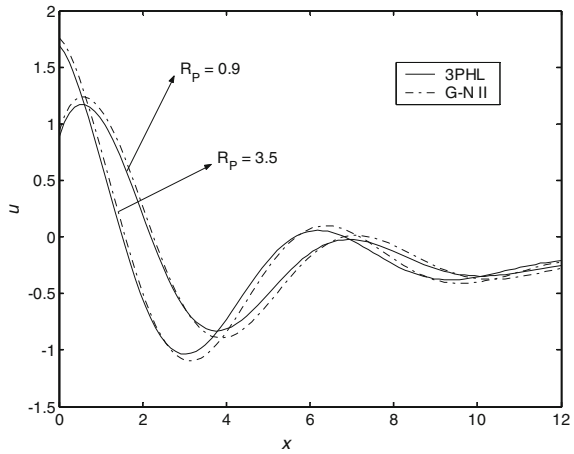

Fig. 1 Horizontal displacement distribution u for two different values of a hydrostatic initial stress

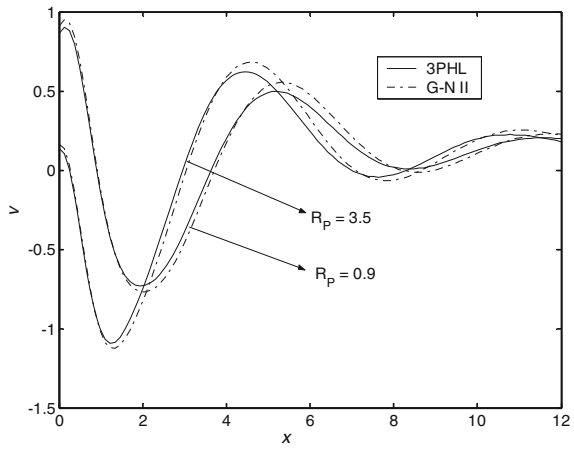

Fig. 2 Vertical displacement distribution v for two different values of a hydrostatic initial stress

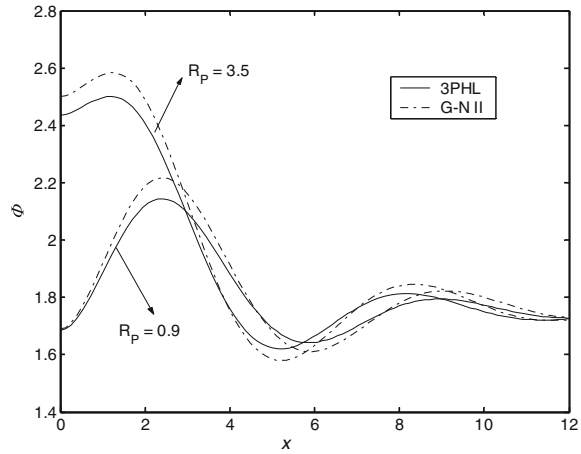

Fig. 3 Conductive temperature distribution Φ for two different values of a hydrostatic initial stress

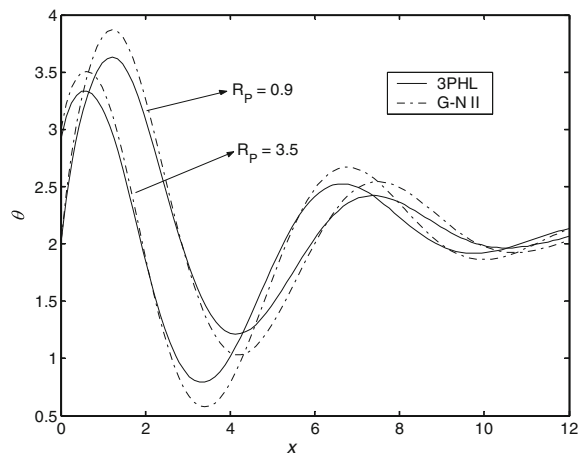

Fig. 4 Thermal temperature distribution θ for two different values of a hydrostatic initial stress

The computations were carried out for a value of time $t = 0.9$. The variations of the thermal temperature θ, the conductive temperature Φ, the displacement components u, v, and the stress components σ_{xx}, σ_{zz}, σ_{xz} with distance x for the value of z, namely $z = -1$, were substituted in performing the computation. The results are shown in Figs. 1, 2, 3, 4, 5, 6, 7, 8, 9, 10, 11, 12, 13, 14, 15, 16, 17, 18, 19, 20, and 21. The graphs show the four curves predicted by the two different models of thermoelasticity. In these figures, the solid lines represent the solution in the **3PHL** model and the dashed lines represent the solution derived using the thermoelasticity without energy dissipation (**G-N II**) theory. Here all the variables are taken in non-dimensional forms and we consider five cases

1. The corresponding equations for a two-temperature generalized-magneto thermoelastic medium in the presence of the rotation ($\Omega = 2.5$) for two different values of a hydrostatic initial stress from the above mentioned cases by taking $R_P = 0.9, 3.5$.
2. The corresponding equations for a two-temperature generalized-magneto thermoelastic

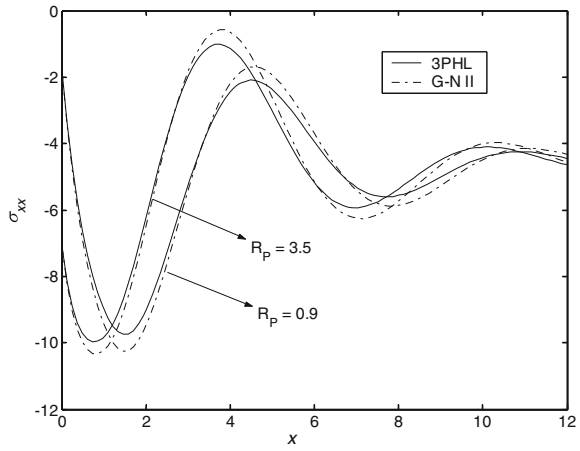

Fig. 5 Distribution of stress component σ_{xx} for two different values of a hydrostatic initial stress

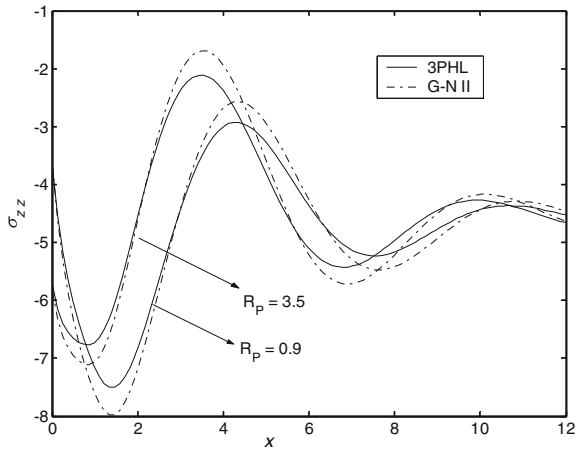

Fig. 7 Distribution of stress component σ_{zz} for two different values of a hydrostatic initial stress

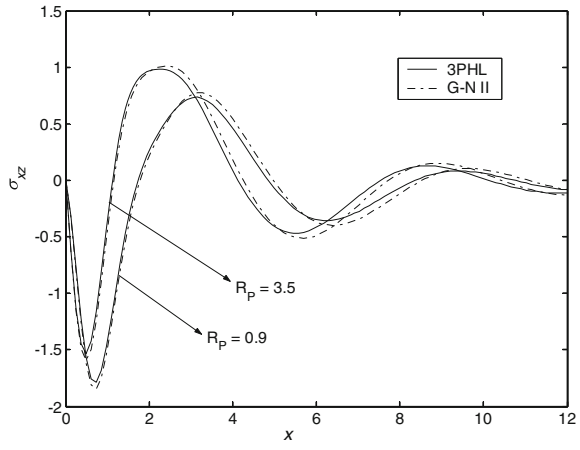

Fig. 6 Distribution of stress component σ_{xz} for two different values of a hydrostatic initial stress

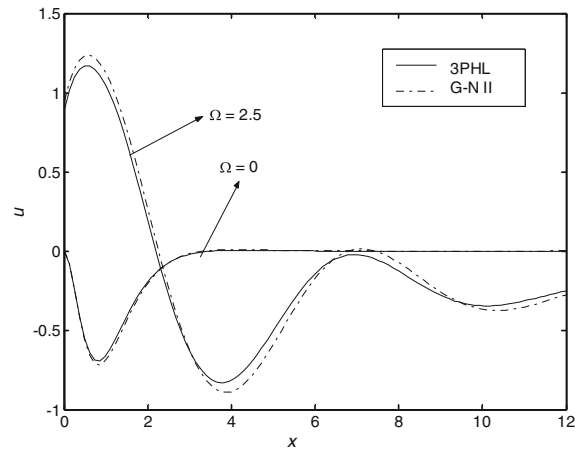

Fig. 8 Horizontal displacement distribution u in the absence and presence of rotation

medium in the presence of a hydrostatic initial stress ($R_P = 0.9$) and in the absence of a rotation from the above mentioned cases by taking Ω to vanish.

3. The corresponding equations for a generalized-magneto thermoelastic medium in the presence of a hydrostatic initial stress ($R_P = 0.9$) and a rotation ($\Omega = 2.5$) from the above mentioned cases by taking δ to vanish.
4. Equations of the **3PHL** model when $K, \tau_T, \tau_q, \tau_v > 0$, and the solutions are always (exponentially) stable if $\frac{2K\tau_T}{\tau_q} > \tau_v^* > K^*\tau_q$ as in [11].
5. Equations of the thermoelasticity without energy dissipation **(G-N II)** theory when $K = \tau_T = \tau_q = \tau_v = 0$.

Figures 1, 2, 3, 4, 5, 6 and 7 show comparisons between the displacement components u, v, the thermal temperature θ, the conductive temperature Φ, and the stress components σ_{xx}, σ_{zz}, σ_{xz} for two different values of a hydrostatic initial stress ($R_P = 0.9,\ 3.5$) with two-temperature and in the presence of rotation ($\Omega = 2.5$).

Figure 1 depicts that the distribution of the horizontal displacement u begins from positive values. In the context of the two models, u starts with

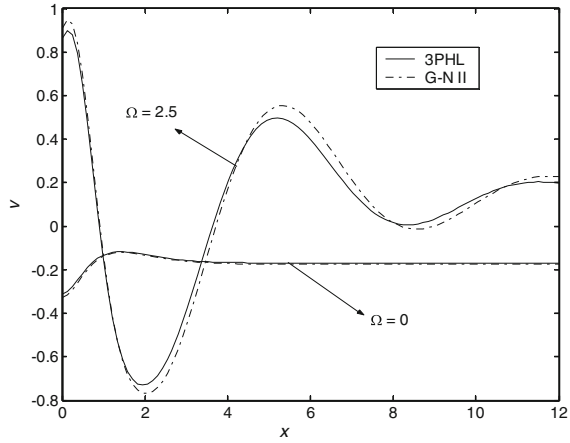

Fig. 9 Vertical displacement distribution v in the absence and presence of rotation

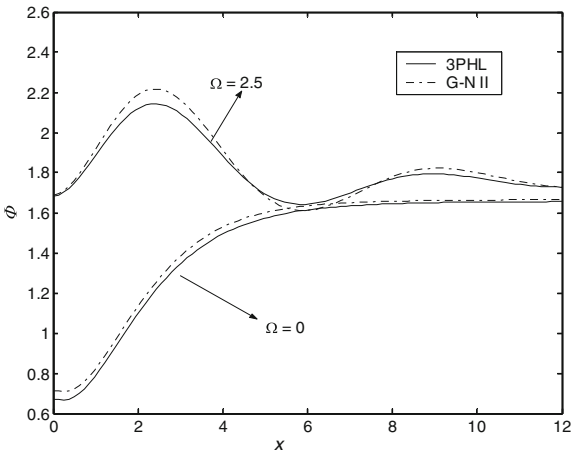

Fig. 10 Conductive temperature distribution Φ in the absence and presence of rotation

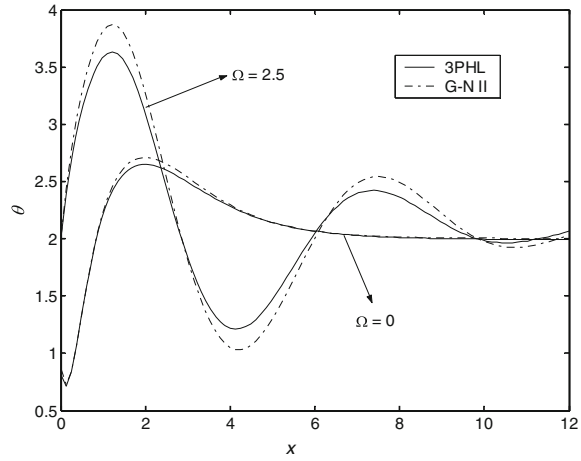

Fig. 11 Thermal temperature distribution θ in the absence and presence of rotation

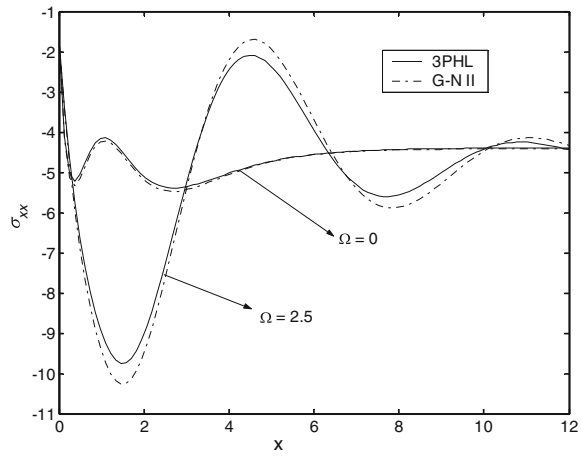

Fig. 12 Distribution of stress component σ_{xx} in the absence and presence of rotation

increasing to a maximum value in the range $0 \leq x \leq 0.8$, then decreases to a minimum value in the range $0.8 \leq x \leq 3.9$, and also moves in a wave propagation for $R_P = 0.9$. However, in the context of the two models, u starts with decreasing to a minimum value in the range $0 \leq x \leq 3$, then increases in the range $3 \leq x \leq 6$, and also moves in a wave propagation for $R_P = 3.5$. The values of u increase with increasing the magnitude of a hydrostatic initial stress in the first, then decrease, again increase and so on. Figure 2 exhibits that the distribution of the vertical displacement v begins from positive values. In the context of the two models, v starts with increasing to a maximum value in the range $0 \leq x \leq 0.1$, then decreases to a minimum value in the range $0.1 \leq x \leq 2$, and also moves in a wave propagation for $R_P = 0.9$. However, in the context of the two models, v starts with decreasing to a minimum value in the range $0 \leq x \leq 1.5$, then increases to a maximum value in the range $1.5 \leq x \leq 4.4$, and also moves in a wave propagation for $R_P = 3.5$. The values of v decrease with increasing the magnitude of a hydrostatic initial stress in the first, then increase, again decrease and so on. The displacement components u and v show different behaviors, because the elasticity of the solid tends to resist a vertical displacement in the problem under the investigation. It is clear from Fig. 3 that the

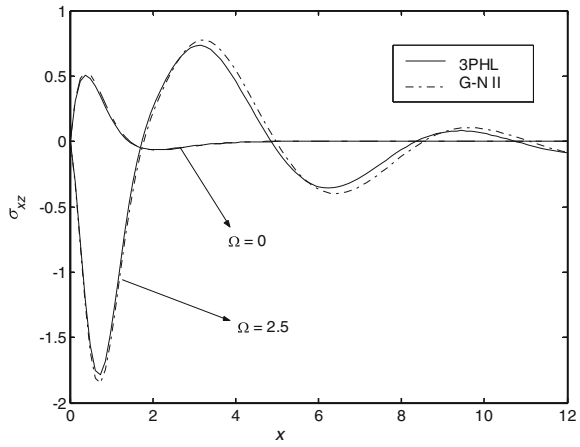

Fig. 13 Distribution of stress component σ_{xz} in the absence and presence of rotation

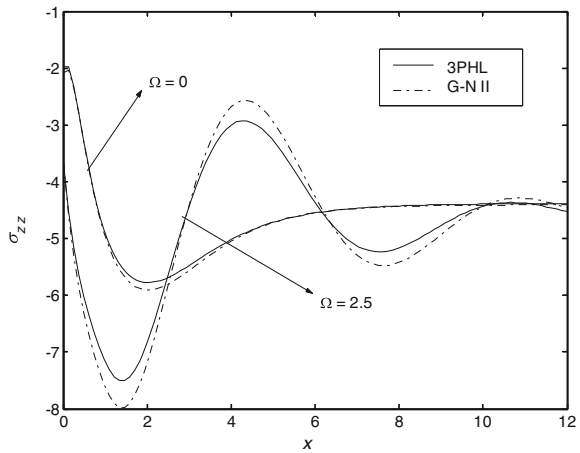

Fig. 14 Distribution of stress component σ_{zz} in the absence and presence of rotation

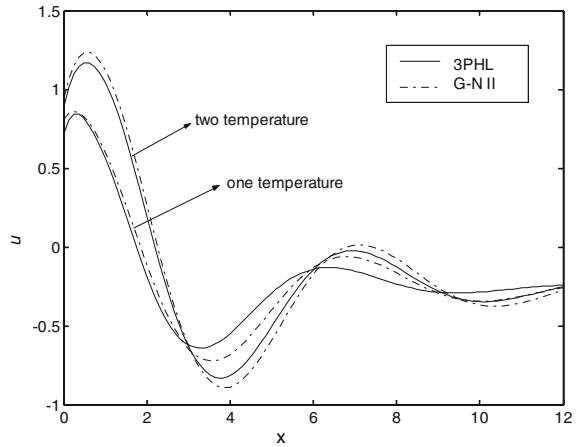

Fig. 15 Horizontal displacement distribution u in the absence and presence of two-temperature parameter

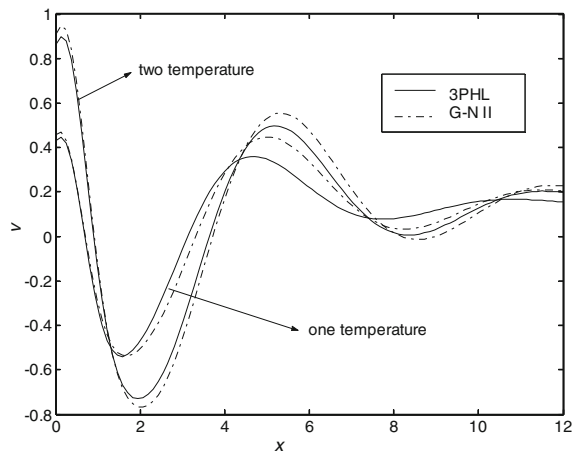

Fig. 16 Vertical displacement distribution v in the absence and presence of two-temperature parameter

conductive temperature Φ begins from positive values. In the context of the two models, Φ starts with increasing to a maximum value in the range $0 \leq x \leq 2.2$, then decreases in the range $2.2 \leq x \leq 6$, and also moves in a wave propagation for $R_P = 0.9$. However, in the context of the two models, Φ starts with increasing to a maximum value in the range $0 \leq x \leq 1.8$, then decreases to a minimum value in the range $1.8 \leq x \leq 5.5$, and also moves in a wave propagation for $R_P = 3.5$. The values of Φ increase with increasing the magnitude of a hydrostatic initial stress in the first, then decrease, again increase and so on. It is clear from Fig. 4 that the thermal temperature θ begins from positive values. In the context of the two models, θ starts with increasing to a maximum value, then decreases to a minimum value, and also moves in a wave propagation for $R_P = 0.9,\ 3.5$. The values of θ increase with increasing the magnitude of a hydrostatic initial stress in the first, then decrease, again increase and so on. Figure 5 displays that the distribution of the stress component σ_{xx} begins from negative values and satisfies the boundary condition at $x = 0$. In the context of the two models, σ_{xx} starts with decreasing to a minimum value, then increases to a maximum value, and also moves in a wave propagation for $R_P = 0.9,\ 3.5$. Fig. 6 shows the distribution of the stress component σ_{xz} and demonstrates that it reaches a zero value and satisfies the

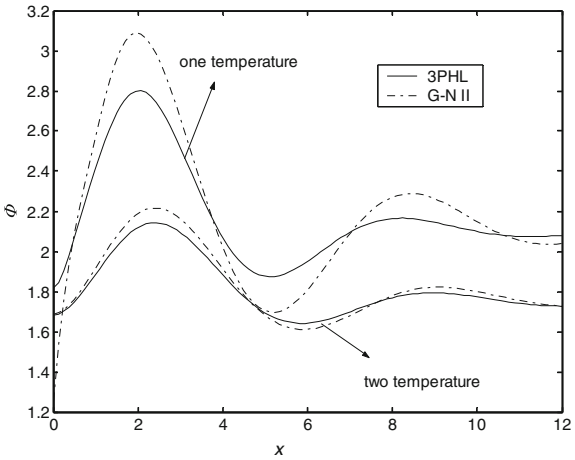

Fig. 17 Conductive temperature distribution Φ in the absence and presence of two-temperature parameter

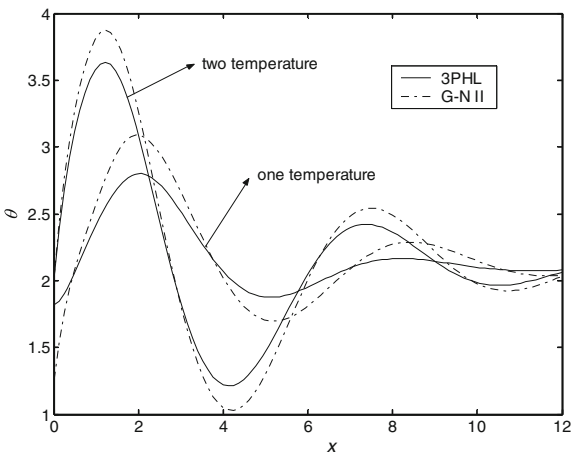

Fig. 18 Thermal temperature distribution θ in the absence and presence of two-temperature parameter

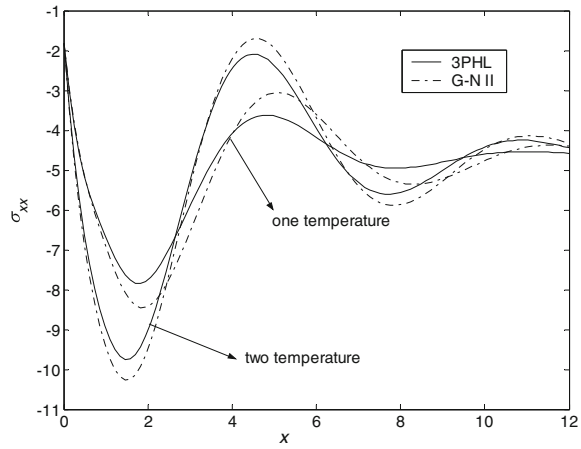

Fig. 19 Distribution of stress component σ_{xx} in the absence and presence of two-temperature parameter

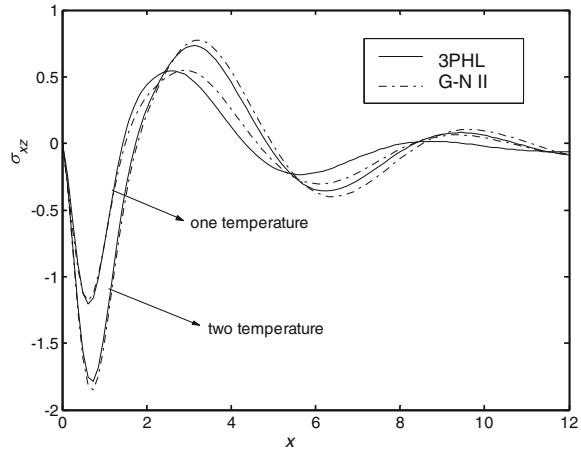

Fig. 20 Distribution of stress component σ_{xz} in the absence and presence of two-temperature parameter

boundary condition at $x = 0$. In the context of the two models, σ_{xz} starts with decreasing to a minimum value, then increases to a maximum value, and also moves in a wave propagation for $R_P = 0.9, 3.5$. Fig. 7 depicts that the distribution of the stress componentσ_{zz} begins from negative values. In the context of the two models, σ_{zz} starts with decreasing to a minimum value, then increases to a maximum value, and also moves in a wave propagation for $R_P = 0.9, 3.5$. The values of stress components σ_{xx}, σ_{zz}, σ_{xz} decrease with increasing the magnitude of a hydrostatic initial stress in the first, then increase, again decrease and so on. Figures 1, 2, 3, 4, 5, 6 and 7 demonstrate that the hydrostatic initial stress has a significant role on all the physical quantities.

Figures 8, 9, 10, 11, 12, 13 and 14 show comparisons between the displacement components u, v, the thermal temperature θ, the conductive temperature Φ, and the stress components σ_{xx}, σ_{zz}, σ_{xz} in the absence ($\Omega = 0$) and presence ($\Omega = 2.5$) of the rotation with two-temperature and in the presence of a hydrostatic initial stress ($R_P = 0.9$).

Figure 8 depicts that the distribution of the horizontal displacement u begins from positive values for $\Omega = 2.5$, but it begins from a zero value for $\Omega = 0$. In the context of the two models, u starts with decreasing to a minimum value in the range

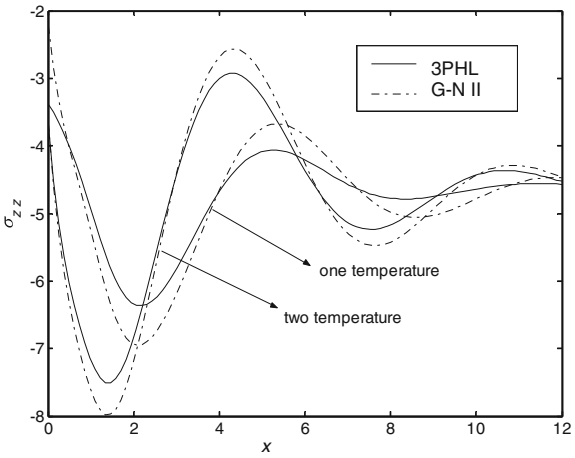

Fig. 21 Distribution of stress component σ_{zz} in the absence and presence of two-temperature parameter

$0 \leq x \leq 0.9$, then increases in the range $0.9 \leq x \leq 4$, and in the last becomes nearly constant for $\Omega = 0$. The values of u increase in the presence of the rotation in the first, then decrease in the last. Figure 9 exhibits that the distribution of the vertical displacement v begins from positive values for $\Omega = 2.5$, but it begins from negative values for $\Omega = 0$. In the context of the two models, v starts with increasing to a maximum value in the range $0 \leq x \leq 1.8$, then decreases in the range $1.8 \leq x \leq 4$, and in the last becomes nearly constant for $\Omega = 0$. The values of v increase in the presence of the rotation in the first, then decrease, and in the last increase. It is clear from Fig. 10 that the conductive temperature Φ begins from positive values. In the context of the two models, Φ increases in the range $0 \leq x \leq 12$ for $\Omega = 0$. The values of Φ increase in the presence of the rotation. It is clear from Fig. 11 that the thermal temperature θ begins from positive values. In the context of the two models, θ starts with decreasing to a minimum value, then increases to a maximum value, and in the last decreases for $\Omega = 0$. The values of θ increase in the presence of the rotation in the first, then decrease, and in the last increase. Figure 12 displays that the distribution of the stress component σ_{xx} begins from a negative value and satisfies the boundary condition at $x = 0$. In the context of the two models, σ_{xx} starts with decreasing, then increases, again decreases, and in the last increases for $\Omega = 0$. Fig. 13 shows the distribution of the stress componentσ_{xz} and demonstrates that it reaches a zero value and satisfies the boundary condition at $x = 0$. In the context of the two models, σ_{xz} starts with increasing to a maximum value, then decreases, and in the last becomes nearly constant for $\Omega = 0$. Fig. 14 depicts that the distribution of the stress component σ_{zz} begins from negative values. In the context of the two models, σ_{zz} starts with decreasing to a minimum value, then increases, and in the last becomes nearly constant for $\Omega = 0$. The values of stress components σ_{xx}, σ_{zz}, σ_{xz} decrease in the presence of the rotation in the first, then increase, again decrease, and the last increase. Figures 8, 9, 10, 11, 12, 13 and 14 explain that in the absence of the rotation all the physical quantities have different behavior and the rotation has an important effect on all the physical quantities.

Figures 15, 16, 17, 18, 19, 20 and 21 show comparisons between the displacement components u, v, the thermal temperature θ, the conductive temperature Φ, the stress components σ_{xx}, σ_{zz}, σ_{xz} with one $(\delta = 0)$ and two $(\delta = 3 \times 10^{-15})$ temperatures in the presence of rotation $(\Omega = 2.5)$ and a hydrostatic initial stress $(R_P = 0.9)$.

Figure 15 depicts that the distribution of the horizontal displacement u begins from positive values. In the context of the two models, u starts with increasing to a maximum value, then decreases to a minimum value, and also moves in a wave propagation for $\delta = 0$. Fig. 16 exhibits that the distribution of the vertical displacement v begins from positive values. In the context of the two models, v starts with increasing to a maximum value, then decreases to a minimum value, and also moves in a wave propagation for $\delta = 0$. The values of displacement components u, v increase in the presence of the two-temperature parameter in the first, then decrease, again increase, and so on. It is clear from Fig. 17 that the conductive temperature Φ begins from positive values. In the context of the two models, Φ starts with increasing to a maximum value, then decreases, and also moves in a wave propagation for $\delta = 0$. The values of Φ decrease in the presence of the two-temperature parameter. It is clear from Fig. 18 that the thermal temperature θ begins from positive values. In the context of the two models, θ starts with increasing to a maximum value, then decreases, and also moves in a wave propagation for $\delta = 0$. The values of θ increase in the presence of the two-temperature

parameter in the first, then decrease, again increase, and so on. Figure 19 displays that the distribution of the stress component σ_{xx} begins from a negative value and satisfies the boundary condition at $x = 0$. In the context of the two models, σ_{xx} starts with decreasing to a minimum value, then increases, and also moves in a wave propagation for $\delta = 0$. Fig. 20 shows the distribution of the stress component σ_{xz} and demonstrates that it reaches a zero value and satisfies the boundary condition at $x = 0$. In the context of the two models, σ_{xz} starts with decreasing to a minimum value, then increases to a maximum value, and also moves in a wave propagation for $\delta = 0$. Fig. 21 depicts that the distribution of the stress component σ_{zz} begins from negative values. In the context of the two models, σ_{zz} starts with decreasing to a minimum value, then increases, and also moves in a wave propagation for $\delta = 0$. The values of stress components σ_{xx}, σ_{zz}, σ_{xz} decrease in the presence of the two-temperature parameter in the first, then increase, again decrease, and so on. Figures 15, 16, 17, 18, 19, 20 and 21 demonstrate that the two-temperature parameter has a significant role on all the physical quantities.

6 Conclusion

In the present study, normal mode analysis is used to study the effect of the rotation and the hydrostatic initial stress on the problem under consideration at the free surface of a two-temperature generalized-magneto thermoelastic medium with an internal heat source that is moving with a constant speed based on the **3PHL** model and the **G-N II** theory. We obtain the following conclusions based on the above analysis:

1. The values of all the physical quantities converge to zero with increasing distance x, and all functions are continuous.
2. Deformation of a generalized thermoelastic medium depends on the nature of the applied force as well as the type of boundary conditions.
3. Analytical solutions based upon normal mode analysis of the thermoelastic problem in solids have been developed and utilized.
4. There are significant differences in the field quantities under the **G-N II** theory and **3PHL** model due to the phase-lag of temperature gradient and the phase-lag of heat flux.
5. All the physical quantities satisfy the boundary conditions.
6. It is clear that the rotation and hydrostatic initial stress (R_P) play significant roles on all the physical quantities.
7. The two-temperature has great influence on the distribution of all physical quantities.
8. Three-phase-lag model is a mathematical model that includes the heat flux vector, the temperature gradient and the thermal displacement gradient, which are useful in the problems of heat transfer, heat conduction, nuclear boiling, exothermic catalytic reactions, phonon-electron interactions, phonon-scattering. So the 3PHL model is the most adequate theory to describe the present problem.
9. The curves in the context of the **3PHL** model and the **G-N II** theory, decrease exponentially with increasing x; this indicates that the thermoelastic waves are unattenuated and non-dispersive, while purely thermoelastic waves undergo both attenuation and dispersion.

References

1. Biot MA (1956) Thermoelasticity and irreversible thermodynamics. J Appl Phys 27:240–253
2. Lord HW, Shulman Y (1967) A generalized dynamical theory of thermo-elasticity. J Mech Phys Solid 15:299–309
3. Green AE, Lindsay KA (1972) Thermoelasticity. J Elast 2:1–7
4. Hetnarski RB, Ignaczak J (1994) Generalized thermoelasticity: response of semi-space to a short laser pulse. J Therm Stress 17:377–396
5. Green AE, Naghdi PM (1991) A re-examination of the basic postulate of thermo-mechanics. Proc R Soc Lond 432:171–194
6. Green AE, Naghdi PM (1992) On undamped heat waves in an elastic solid. J Therm Stress 15:253–264
7. Green AE, Naghdi PM (1993) Thermoelasticity without energy dissipation. J Elast 31:189–208
8. Tzou DY (1995) A unified approach for heat conduction from macro-to micro-scales. ASME J Heat Transf 117:8–16
9. Chandrasekharaiah DS (1998) Hyperbolic thermoelasticity: a review of recent literature. J Appl Mech Rev 51:705–729
10. Choudhuri SR (2007) On a thermoelastic three-phase-lag model. J Therm Stress 30:231–238
11. Quintanilla R, Racke R (2008) A note on stability in three-phase-lag heat conduction. Int J Heat Mass Transf 51:24–29
12. Kar A, Kanoria M (2009) Generalized thermo-visco-elastic problem of a spherical shell with three-phase-lag effect. J Appl Math Model 33:3287–3298

13. Quintanilla R (2009) Spatial behaviour of solutions of the three-phase-lag heat equation. J Appl Math Comput 213: 153–162
14. Kanoria M, Mallik SH (2010) Generalized thermoviscoelastic interaction due to a periodically varying heat source with three-phase-lag effect. Eur J Mech A Solids 29:695–703
15. Abbas IA (2014) Three-phase lag model on thermoelastic interaction in an unbounded fiber-reinforced anisotropic medium with a cylindrical cavity. J Comput Theor Nanosci 11:987–992
16. Othman MIA, Said SM (2014) 2D problem of magneto-thermoelasticity fiber-reinforced medium under temperature dependent properties with three-phase-lag model. J Mecc 49:1225–1241
17. Chen PJ, Gurtin ME (1968) On a theory of heat conduction involving two temperatures. Z Angew Math Phys 19: 614–627
18. Chen PJ, Gurtin ME, Williams WO (1968) A note on non simple heat conduction. Z Angew Math Phys 19:969–970
19. Chen PJ, Gurtin ME, Williams WO (1969) On the thermodynamics of non-simple elastic materials with two-temperatures. Z Angew Math Phys 20:107–112
20. Warren WE, Chen PJ (1973) Wave propagation in the two temperatures theory of thermoelasticity. J Acta Mech 16:21–33
21. Youssef HM (2005) Theory of two-temperature generalized thermoelasticity. IMA J Appl Math 71:383–390
22. Puri P, Jordan PM (2006) On the propagation of harmonic plane wanes under the two temperature theory. Int J Eng Sci 44:1113–1126
23. Abbas IA, Youssef HM (2009) Finite element method of two-temperature generalized magneto-thermoelasticity. J Arch Appl Mech 79:917–925
24. Kumar R, Mukhopadhyay S (2010) Effects of thermal relaxation time on plane wave propagation under two-temperature thermoelasticity. Int J Eng Sci 48:128–139
25. Das P, Kanoria M (2012) Two-temperature magneto-thermo-elastic response in a perfectly conducting medium based on GN-III model. Int J Pure Appl Math 81:199–229
26. Abbas IA, Zenkour AM (2014) Two-temperature generalized thermoplastic interaction in an infinite fiber-reinforced anisotropic plate containing a circular cavity with two relaxation times. J Comput Theor Nanosci 11:1–7
27. Othman MIA, Hasona WM, Abd-Elaziz EM (2014) Effect of rotation on micropolar generalized thermoelasticity with two temperatures using a dual-phase lag model. Can J Phys 92:149–158
28. Chand D, Sharma JN, Sud SP (1990) Transient generalized magneto thermo-elastic waves in a rotating half-space. Int J Eng Sci 28:547–556
29. Choudhuri SKR, Roy GC (1990) Temperature-rate dependent magneto-thermoelastic waves in a finitely conducting elastic half-space. J Comput Math Appl 19:85–93
30. Ezzat MA, Othman MIA (2000) Electromagneto-thermoelastic plane waves with two relaxation times in a medium of perfect conductivity. Int J Eng Sci 38:107–120
31. Othman MIA, Song YQ (2008) Effect of rotation on plane waves of the generalized electro magneto-thermo-viscoelasticity with two relaxation times. J Appl Math Model 32:811–825
32. Othman MIA, Said SM (2013) Plane waves of a fiber-reinforcement magneto-thermoelastic comparison of three different theories. Int J Thermophys 34:366–383
33. Montanaro A (1999) On singular surface in isotropic linear thermoelasticity with initial stress. J Acoust Soc Am 106:1586–1588
34. Ahmed SM (2000) Rayleigh waves in a thermoelastic granular medium under initial stress. Int J Math Math Sci 23:627–637
35. Othman MIA, Said SM (2012) The effect of mechanical force on generalized thermoelasticity in a fiber-reinforced under three theories. Int J Thermophys 33:1082–1099
36. Schoenberg M, Censor D (1973) Elastic waves in rotating media. J Quart Appl Math 31:115–125